

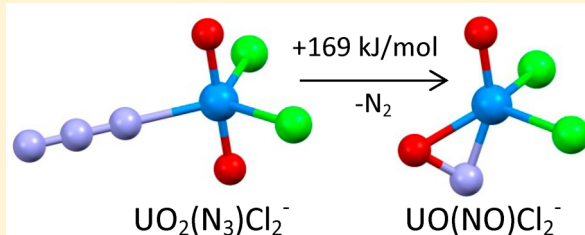
Gas Phase Uranyl Activation: Formation of a Uranium Nitrosyl Complex from Uranyl Azide

Yu Gong,[†] Wibe A. de Jong,^{*,‡} and John K. Gibson^{*,†}

[†]Chemical Sciences Division, [‡]Computational Research Division, Lawrence Berkeley National Laboratory, Berkeley, California 94720, United States

S Supporting Information

ABSTRACT: Activation of the oxo bond of uranyl, UO_2^{2+} , was achieved by collision induced dissociation (CID) of $\text{UO}_2(\text{N}_3)\text{Cl}_2^-$ in a quadrupole ion trap mass spectrometer. The gas phase complex $\text{UO}_2(\text{N}_3)\text{Cl}_2^-$ was produced by electrospray ionization of solutions of UO_2Cl_2 and NaN_3 . CID of $\text{UO}_2(\text{N}_3)\text{Cl}_2^-$ resulted in the loss of N_2 to form $\text{UO}(\text{NO})\text{Cl}_2^-$, in which the “inert” uranyl oxo bond has been activated. Formation of UO_2Cl_2^- via N_3 loss was also observed. Density functional theory computations predict that the $\text{UO}(\text{NO})\text{Cl}_2^-$ complex has nonplanar C_2 symmetry and a singlet ground state. Analysis of the bonding of the $\text{UO}(\text{NO})\text{Cl}_2^-$ complex shows that the side-on bonded NO moiety can be considered as NO^{3-} , suggesting a formal oxidation state of U(VI). Activation of the uranyl oxo bond in $\text{UO}_2(\text{N}_3)\text{Cl}_2^-$ to form $\text{UO}(\text{NO})\text{Cl}_2^-$ and N_2 was computed to be endothermic by 169 kJ/mol, which is energetically more favorable than formation of NUOCl_2^- and UO_2Cl_2^- . The observation of UO_2Cl_2^- during CID is most likely due to the absence of an energy barrier for neutral ligand loss.



INTRODUCTION

Activation and functionalization of the oxo bond in UO_2^{2+} has attracted much attention as a result of the importance of this species and these particular bonds for understanding the fundamental chemistry of uranium and for developing strategies for separations processes.^{1–3} Progress in this endeavor has been made despite difficulties in achieving chemical transformation of the chemically inert U–O bonds in uranyl.⁴ Reductive silylation^{5–8} and coordination by Lewis acids such as alkali metals and $\text{B}(\text{C}_6\text{F}_5)_3$ to the yl oxygen of uranyl^{9–11} are the primary routes that have been developed in the condensed phase; the U–O bond is reduced during these processes.

The success in uranyl activation initiated interest in exploring similar chemistry in the gas phase, where uranyl complexes can be studied without interferences present in condensed phase. A study of the reaction of UO_2^+ and H_2^{18}O revealed yl oxygen exchange in the gas phase, which has been previously observed in solution.¹² Similar results were observed for exchange of uranyl with $\text{CH}_3^{18}\text{OH}$.¹³ The exchange mechanisms were evaluated by density functional theory (DFT) in both of these studies.^{12,13} In contrast to oxo-exchange, where no net reaction occurs, the fragmentation chemistry of $\text{UO}_2(\text{NCO})\text{Cl}_2^-$ demonstrated that novel uranium containing molecules can be made via gas phase activation of uranyl.¹⁴ It was found that collision induced dissociation (CID) of $\text{UO}_2(\text{NCO})\text{Cl}_2^-$ prepared via electrospray ionization (ESI) resulted in elimination of CO_2 and the formation of NUOCl_2^- , in which one of the terminal oxo bonds has been replaced by a nitrido bond. The observation of such a reaction not only demonstrated a new route to uranyl activation but also

provided a rare example of the formation of a nitrido complex from uranyl; such uranium nitridos have been prepared previously in gas and condensed phases only by oxidation reactions of low-valent and atomic uranium.^{15–20} The coupling between NCO^- and an yl oxygen under CID conditions raises the possibility that the isoelectronic azide ligand, N_3^- , can similarly induce uranyl activation. Azides are known to serve as precursors for the synthesis of metal nitrides, as in the recent preparation of the first uranium compound bearing a terminal U–N triple bond.^{20,21} Reported here are results for CID of the $\text{UO}_2(\text{N}_3)\text{Cl}_2^-$ complex. Formation of $\text{UO}(\text{NO})\text{Cl}_2^-$ via N_2 loss is observed, with the uranium complex characterized by DFT as a UOCl_2^- moiety with uranium coordinated by a side-on bonded NO ligand. Loss of N_3 to form UO_2Cl_2^- is also a major fragmentation channel upon CID of $\text{UO}_2(\text{N}_3)\text{Cl}_2^-$.

EXPERIMENTAL AND THEORETICAL METHODS

All the experiments were performed using an Agilent 6340 quadrupole ion trap mass spectrometer (QIT/MS) with the electrospray ionization (ESI) source inside a radiological contaminant glovebox, as described in detail elsewhere.²² The $\text{UO}_2(\text{N}_3)\text{Cl}_2^-$ anion was produced by ESI of methanol solutions containing UO_2Cl_2 and NaN_3 ($\text{UO}_2\text{Cl}_2/\text{NaN}_3 \approx 1:5$, 200 μM UO_2Cl_2). The MS^n CID capabilities of the QIT/MS allow isolation and fragmentation of ions with a particular mass-to-charge ratio, m/z . CID under these experimental conditions is achieved by multiple low-energy collisions of the selected ion with helium atoms. In contrast to high-energy single-collision CID,

Received: August 19, 2014

Revised: March 6, 2015

Published: April 23, 2015

this approach essentially results in heating of the complex ion until an effective temperature distribution is reached that enables fragmentation into one or more product ions. Because the ions are gradually heated there is necessarily an energy distribution and it is common to observe two or more product ions that exhibit similar barriers to fragmentation; only in cases where one fragmentation channel is much lower in energy than all others is a single CID product observed. In high resolution mode, the instrument has a detection range of 20–2200 m/z with a mass width (fwhm) of $\sim 0.3 m/z$. Mass spectra were recorded in the negative ion accumulation and detection mode. The parameters used to obtain experimental spectra were similar to those reported previously.¹⁴ High-purity nitrogen gas for nebulization and drying in the ion transfer capillary was supplied from the boil-off from a liquid nitrogen Dewar. As has been discussed elsewhere,^{23–25} the background water and O₂ pressures in the ion trap are estimated to be on the order of 10⁻⁶ Torr. The helium buffer gas pressure in the trap is constant at $\sim 10^{-4}$ Torr.

The electronic structure energy calculations and geometry optimizations were performed at the DFT level of theory using the hybrid gradient corrected PBE0²⁶ exchange correlation functional. An unrestricted wave function was used for all open-shell DFT calculations. Multiple electronic states and starting geometries were probed to find the ground state configuration of each species. The Effective Core Potentials (ECPs) and Gaussian basis sets of Dolg et al. were employed for U^{27,28} while the aug-cc-pVTZ basis sets of Dunning were used for O, N, and Cl.^{29–31} Zero-point energy corrections were included in the calculated energies. All electronic structure calculations in this study were performed using NWChem computational chemistry software.³²

RESULTS AND DISCUSSION

The ESI mass spectrum of methanol solutions of UO₂Cl₂ and NaN₃ resulted in formation of three uranyl azide complexes, UO₂(N₃)Cl₂⁻, UO₂(N₃)₂Cl⁻, and UO₂(N₃)₃⁻; the relative abundance of UO₂(N₃)Cl₂⁻ increases as the NaN₃/UO₂Cl₂ concentration ratio increases. In addition, sodium azide chloride anions in the form of Na_x(N₃)_yCl_{x-y+1}⁻ were produced upon ESI. The UO₂(N₃)Cl₂⁻ complex with two chloride ligands was chosen for study to avoid potential coupling between N₃ ligands during CID. Mass selection and CID of UO₂(N₃)Cl₂⁻ at m/z 382, which is the most abundant isotopomer, UO₂(N₃)³⁵Cl₂⁻, resulted in the appearance of two peaks, at m/z 340 and 354 (Figure 1). The m/z 340 peak corresponds to UO₂Cl₂⁻ from loss of neutral N₃ from UO₂(N₃)Cl₂⁻, with reduction of U(VI) to U(V). The m/z 354 peak is more intriguing, as it corresponds to loss of N₂ from UO₂(N₃)Cl₂⁻, indicating the formation of a complex with composition UO₂NCl₂⁻. Since the U–Cl bond is much

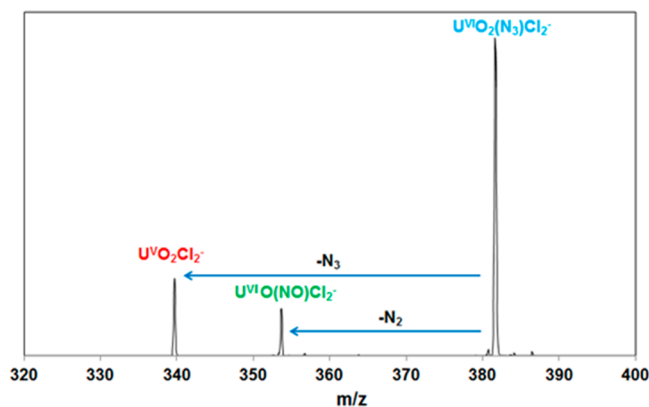


Figure 1. CID spectrum of UO₂(N₃)Cl₂⁻.

stronger than N–Cl and O–Cl bonds,³³ both chlorine atoms should remain bound to uranium. Hence, the most plausible structure of UO₂NCl₂⁻ is a uranium monoxide complex coordinated by molecular NO, [UO(NO)Cl₂]⁻, which would result from activation of a uranyl U–O bond.

DFT calculations were employed to identify the ground state structures of the precursor complex UO₂(N₃)Cl₂⁻, its observed CID products UO₂NCl₂⁻ and UO₂Cl₂⁻, and UONCl₂⁻ that would have resulted from N₂O elimination. The lowest energy structures are shown in Figure 2, the geometrical parameters

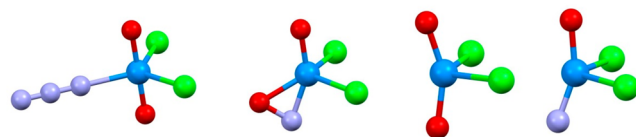


Figure 2. Optimized structures of UO₂(N₃)Cl₂⁻, UO(NO)Cl₂⁻, UO₂Cl₂⁻, and NUOCl₂⁻. The geometrical parameters are given in Table 1. The structure of UO(NO)Cl₂⁻ is I in Figure 3.

are given in Table 1, and the vibrational frequencies associated with the uranium–oxygen and uranium–nitrogen bonds are given in Table 2. The precursor complex UO₂(N₃)Cl₂⁻ has a singlet ground state representing a U(VI) species, with a triplet state over 200 kJ/mol higher in energy. The results for UONCl₂⁻ are in agreement with those previously reported using DFT-B3LYP/SDD.¹⁴ All structures that could be reasonably formed from UO(NO)Cl₂⁻ were explored within the unrestricted DFT framework with singlet, open-shell singlet, and triplet spin states. The full set of optimized geometries and energetics has been provided as Supporting Information. The two lowest energy structures are two stable isomers with C_s symmetry. Both isomers have one terminal oxo and two chloro ligands, and a NO moiety bound to uranium in a side-on fashion; the difference between the two isomers is the relative positions of two oxygen atoms. Table 3 contains the relative energies, geometrical parameters, and vibrational frequencies for the four lowest-energy structural motifs in various spin states. The four optimized structures UO(NO)Cl₂⁻ are shown in Figure 3. The lower-energy cis isomer (I) exhibits a singlet ground state with an open-shell singlet 13 kJ/mol higher in energy, while the triplet state lies 21 kJ/mol above the singlet ground state. The open-shell singlet state is lowest in energy for the trans isomer (II) with the triplet and singlet state higher in energy by only 6 and 12 kJ/mol, respectively. The singlet cis isomer is 22 kJ/mol lower energy than the open-shell singlet trans isomer. Experimentally observed UO(NO)Cl₂⁻ should exhibit the ground-state singlet cis structure I in Figure 3, in which the O–U–N bond is closer to linear than the O–U–O bond. The open-shell singlet of the linear U–N–O structure (III) is 32 kJ/mol higher in energy relative to the singlet cis isomer. The triplet and singlet linear U–N–O structures were found to be 49 and 84 kJ/mol higher compared to the singlet cis isomer. A triplet C_{2v} structure (IV) representing a uranyl moiety with a nitrogen radical in the equatorial plane is found to be 54 kJ/mol higher in energy. The nitrogen radical in the singlet state was found to have an imaginary mode, which led to the trans isomer discussed above. All other structural motifs considered are found to have energies at least 75 kJ/mol above the singlet cis side-on structure. Additional single-point coupled cluster energy calculations on the two isomers and the linear UNO structure

Table 1. Computed Geometrical Parameters of the Lowest Energy Structure of Each Species Shown in Figure 2^a

Species	U–O	U–N	U–Cl	O–N	O–U–O	O–U–N	O–U–Cl
[UO ₂ (N ₃)Cl ₂] [−]	1.745	2.276	2.626		180	90	90
[UO(NO)Cl ₂] [−]	1.778, 2.055	1.879	2.644	1.436	111	153	95
[UO ₂ Cl ₂] [−]	1.807	–	2.672		154	–	97
[NUOCl ₂] [−]	1.782	1.713	2.655		–	156	93

^aBond lengths are in Å; bond angles are in degrees.

Table 2. Computed Vibrational Parameters of the Lowest Energy Structure of Each Species Shown in Figure 2

Species	Frequency ^a	Assignment
[UO ₂ (N ₃)Cl ₂] [−]	924	Symmetric O–U–O stretch
	1001	Antisymmetric O–U–O stretch
[UO(NO)Cl ₂] [−]	695	U–N stretch (minor U–O stretch)
	915	U–O stretch (minor U–N stretch)
	963	N–O stretch (minor U–O stretch)
[UO ₂ Cl ₂] [−]	842	Symmetric O–U–O stretch
	884	Antisymmetric O–U–O stretch
[NUOCl ₂] [−]	899	U–O stretch (minor U–N stretch)
	1094	U–N stretch (minor U–O stretch)

^aFrequencies in cm^{−1}.

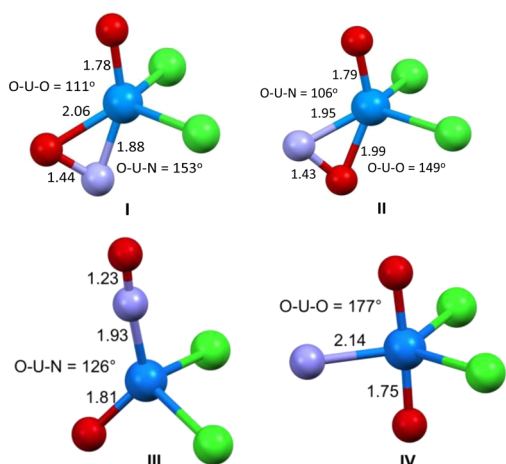


Figure 3. Optimized structures of the cis and trans side-on isomers, the linear UNO, and nitrogen radical structures of [UO(NO)Cl₂][−] at DFT-PBE0 level of theory. Bond lengths are in Å. Structures I–III are for the singlet states, while structure IV is a triplet. More precise bond distances are in Table 3.

confirm the singlet cis isomer to be lowest in energy (see Supporting Information for computational details and energies).

The terminal U–O distance bond in singlet ground state UO(NO)Cl₂[−] is computed to be 1.778 Å, which is similar to the U–O distances (ranging from 1.76 to 1.79 Å) reported in other U(VI) complexes containing UO subunits.^{34,35} The NO ligand bound side-on to uranium in the UO(NO)Cl₂[−] complex is unprecedented. Although transition metal complexes with a side-on bonded NO ligand have been observed previously,³⁶ similar coordination has not been reported for uranium. The first synthesized uranium–NO complex was characterized to have a linear UNO geometry with a N–O bond length of 1.231(5) Å; the NO ligand there was considered to be NO[−] on the basis of various experimental results and DFT calculations.^{37,38} Compared with such a short N–O bond, the rather long N–O bond in the UO(NO)Cl₂[−] complex (1.436 Å) suggests that the NO moiety is significantly further reduced than NO[−] upon coordination to uranium. Evans et al. recently isolated a coordination complex containing a reduced NO^{2−} unit where the NO is sandwiched between two yttrium ions forming a significantly different structural and bonding motif {[(Me₃Si)₂N]₂(THF)Y₂}³⁵(μ-η²:η²-NO) when compared to the uranium species.³⁹ The N–O bond lengths in this compound are 1.346(5) and 1.390(4) Å, somewhat shorter than the N–O bond length found for the singlet state of both isomers of UO(NO)Cl₂[−]. A minus 2 charge and a formal bond order of 1.5 were assigned to the NO in the yttrium complex based on trends in NO stretching frequencies. Natural Bond Orbital (NBO) analysis⁴⁰ of the ground state singlet UO(NO)Cl₂[−] species shows the formation of a U(VI) species where the N–O unit can be described as a NO^{3−} with a single bond and a bond order of 1. Additional DFT calculations and NBO analysis were performed for the yttrium complex to allow for a direct comparison of the bond orders between the yttrium and uranium species. The NBO results confirm the bond order assignment of 1.5 by Evans et al., in contrast to the 1.0 bond order obtained for the singlet UO(NO)Cl₂[−]. In addition to the

Table 3. Computed Geometrical and Vibrational Parameters of [UO(NO)Cl₂][−] Species with Various Spin States within 55 kJ/mol from the Lowest Energy Structure^a

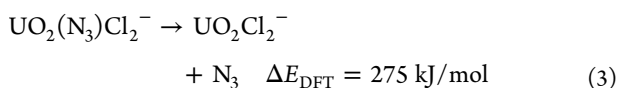
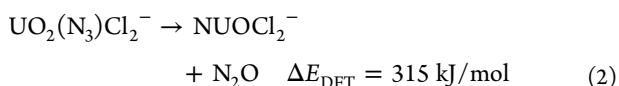
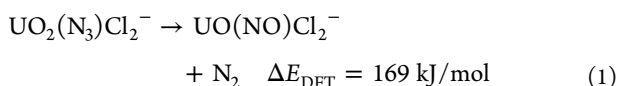
Species	Spin state	Relative energy	U–N	U–O	N–O	Frequency
Cis	Singlet	0	1.879	1.778, 2.055	1.436	911, 962
	Open-shell singlet	13	2.136	1.807, 2.202	1.318	871, 1190
	Triplet	21	2.126	1.803, 2.206	1.316	878, 1190
Trans	Singlet	34	1.949	1.794, 1.993	1.429	886, 966
	Open-shell singlet	22	2.131	1.808, 2.120	1.338	870, 1129
	Triplet	28	2.169	1.807, 2.148	1.324	873, 1163
Linear UNO	Open-shell singlet	32	2.240	1.827	1.207	856, 1677
	Triplet	49	2.200	1.828	1.202	844, 1649
N radical	Triplet	54	2.142	1.754, 1.754	–	900, 983

^aBond lengths are in Å; relative energies in kJ/mol; frequencies in cm^{−1}.

single N–O bond, strong bonds are found between the uranium and the nitrogen (double bond), and the uranium with both oxygen atoms (triple bond for the terminal oxygen and a double bond for the NO oxygen). Comparing the NBO analysis of the higher energy open-shell singlet and the triplet states of both the cis and trans isomers provides additional credence to the U(VI) and NO^{3-} assignment for the ground state singlet cis complex. Both the open-shell singlet and triplet species are found to have an unpaired electron in the *Sf* and an unpaired electron on the NO unit, representing a U(V) and a $(\text{NO})^{2-}$ with a formal bond order of 1.5 as found for the yttrium complex. In addition, note that these electronic states have a N–O bond length that is 0.1 Å shorter than the NO^{3-} proposed for the ground state singlet.

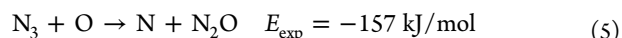
The computed vibrational frequencies of $\text{UO}(\text{NO})\text{Cl}_2^-$ reveal two intense bands at 911 and 962 cm^{-1} (Table 2; see Table S6 in the Supporting Information for calculated intensities) that are in the region where terminal U–O and U–N stretches have been observed.^{41–43} The lower frequency mode is assigned to the U–O stretch for the terminal oxygen, and the higher frequency mode, to the N–O stretch. A U–N dominated stretch with weak intensity was found at 695 cm^{-1} . Compared with the vibrational frequencies for NO ($\sim 1875 \text{ cm}^{-1}$) and NO^- ($\sim 1370 \text{ cm}^{-1}$),⁴⁴ the N–O stretch in the singlet $\text{UO}(\text{NO})\text{Cl}_2^-$ (962 cm^{-1} , Table 3) representing a $(\text{NO})^{3-}$ is much lower. The N–O stretch in the yttrium–NO complex was found to be somewhat lower at 951 cm^{-1} compared to the uranium species studied here. The open-shell singlet and triplet species representing a $(\text{NO})^{2-}$ moiety have a N–O stretch (1190 cm^{-1}) that lies in-between the frequencies of NO^- and the NO^{3-} of the singlet $\text{UO}(\text{NO})\text{Cl}_2^-$. The calculated differences in bond orders, bond lengths, and vibrational frequencies for the ground state singlet when compared to the open-shell singlet and triplet NO^{2-} states provide additional confidence in assigning the U(VI) and NO^{3-} to the ground state singlet species.

Although the N_3^- and NCO^- ligands are isoelectronic, the fragmentation pattern of $\text{UO}_2(\text{N}_3)\text{Cl}_2^-$ upon CID is different from that observed for $\text{UO}_2(\text{NCO})\text{Cl}_2^-$, where loss of CO_2 to form the NUOCl_2^- complex was observed.¹⁴ The difference between the fragmentation chemistries of $\text{UO}_2(\text{N}_3)\text{Cl}_2^-$ and $\text{UO}_2(\text{NCO})\text{Cl}_2^-$ are in accord with the computed energies of three fragmentation channels, reactions 1–3, for the azide complex (ΔE_{DFT} is the computed reaction energy including zero-point corrections).



The optimized geometries of $\text{UO}_2(\text{N}_3)\text{Cl}_2^-$ and the products in reactions 1–3 are in Figure 2 and Table 1. N_2 loss (reaction 1) is energetically the most favorable of the three considered, which accounts for the observation of $\text{UO}(\text{NO})\text{Cl}_2^-$ during CID. Reaction 2 is analogous to the reaction observed for $\text{UO}_2(\text{NCO})\text{Cl}_2^-$ under CID conditions, which would produce NUOCl_2^- ; this channel is computed to be the least favorable,

146 kJ/mol higher in energy than N_2 loss (reaction 1). The different fragmentation behaviors of $\text{UO}_2(\text{NCO})\text{Cl}_2^-$ (CO_2 loss) and $\text{UO}_2(\text{N}_3)\text{Cl}_2^-$ (no N_2O loss) can be related to the comparative energies needed to convert the ligands, NCO or N_3 , to the stable molecules, CO_2 or N_2O , as required for conversion of a U–O bond to a U–N bond; these energies are given by reactions 4 and 5.⁴⁵



Based on the greater exothermicity of reaction 4 versus reaction 5 it is expected that replacement of an O_{yl} by a N atom should be energetically more favorable for the isocyanate ligand than for the azide ligand.

Reaction 3 involves N_3 ligand loss, resulting in the reduction from U(VI) to U(V). Although it is computed to be less favorable than N_2 loss by 106 kJ/mol, the yield of UO_2Cl_2^- (reaction 3) is slightly greater than that of $\text{UO}(\text{NO})\text{Cl}_2^-$ (reaction 1) upon CID. Since ligand loss generally does not require significant activation energies, whereas an energy barrier should hinder N_2 loss, it is reasonable that reaction 1 is less kinetically favorable than reaction 3, despite the fact that it is less endothermic.

CONCLUSIONS

The fragmentation chemistry of $\text{UO}_2(\text{N}_3)\text{Cl}_2^-$ was investigated in the gas phase using quadrupole ion trap mass spectrometry. The $\text{UO}_2(\text{N}_3)\text{Cl}_2^-$ complex was prepared by ESI of methanol solutions containing UO_2Cl_2 and NaN_3 . CID of $\text{UO}_2(\text{N}_3)\text{Cl}_2^-$ resulted in the formation of $\text{UO}(\text{NO})\text{Cl}_2^-$ by N_2 loss and UO_2Cl_2^- by N_3 loss; the N_2 loss channel involves activation of the inert U–O bond. DFT calculations indicate that the $\text{UO}(\text{NO})\text{Cl}_2^-$ complex has a singlet ground state with a side-on bonded NO ligand. Analysis of the bonding shows that the NO ligand in the singlet ground state species can be considered as NO^{3-} , which implies a formal oxidation state of U(VI). In contrast, analysis of the higher energy open-shell singlet and triplet states have an NO ligand that can be considered as NO^{2-} , and a formal oxidation state of U(V). Although formation of $\text{UO}(\text{NO})\text{Cl}_2^-$ from $\text{UO}_2(\text{N}_3)\text{Cl}_2^-$ is endothermic, it is energetically favorable compared with the other two competitive fragmentation channels, N_3 loss and N_2O loss, for which UO_2Cl_2^- and NUOCl_2^- are the respective products. The observation of a substantial yield of UO_2Cl_2^- during CID of $\text{UO}_2(\text{N}_3)\text{Cl}_2^-$ can be attributed to the absence of an energy barrier for the N_3 ligand-loss reaction; this in contrast to an activation barrier for the formation of $\text{UO}(\text{NO})\text{Cl}_2^-$ and N_2 .

ASSOCIATED CONTENT

Supporting Information

Optimized geometries, vibrational modes, and computed energies of all species studied in this work at the DFT level of theory. Computational details and energies of coupled cluster calculations on lowest energy structures from DFT. The Supporting Information is available free of charge on the ACS Publications website at DOI: 10.1021/jacs.5b02420.

AUTHOR INFORMATION

Corresponding Authors

*wadejong@lbl.gov

*jkgibson@lbl.gov

Notes

The authors declare no competing financial interest.

ACKNOWLEDGMENTS

This work was supported by the U.S. Department of Energy, Office of Basic Energy Sciences, Heavy Element Chemistry, at LBNL under Contract No. DE-AC02-05CH11231. Part of the calculations were performed using the Molecular Science Computing Capability in the William R. Wiley Environmental Molecular Science Laboratory, a national scientific user facility sponsored by the U.S. Department of Energy's Office of Biological and Environmental Research and located at the Pacific Northwest National Laboratory, operated for the Department of Energy by Battelle. Some of the calculations were performed using the Oak Ridge Leadership Computing Facility, which is a DOE Office of Science User Facility supported under Contract DE-AC05-00OR22725. An award of computer time was provided by the Innovative and Novel Computational Impact on Theory and Experiment (INCITE) program.

REFERENCES

- (1) Jones, M. B.; Gaunt, A. J. *Chem. Rev.* **2013**, *113*, 1137.
- (2) Baker, R. J. *Chem.—Eur. J.* **2012**, *18*, 16258.
- (3) Fortier, S.; Hayton, T. W. *Coordin. Chem. Rev.* **2010**, *254*, 197.
- (4) Denning, R. G. *J. Phys. Chem. A* **2007**, *111*, 4125.
- (5) Schnaars, D. D.; Wu, G.; Hayton, T. W. *Inorg. Chem.* **2011**, *50*, 9642.
- (6) Arnold, P. L.; Patel, D.; Wilson, C.; Love, J. B. *Nature* **2008**, *451*, 315.
- (7) Berthet, J. C.; Siffredi, G.; Thuery, P.; Ephritikhine, M. *Eur. J. Inorg. Chem.* **2007**, 4017.
- (8) Pedrick, E. A.; Wu, G.; Hayton, T. W. *Inorg. Chem.* **2014**, *53*, 12237.
- (9) Arnold, P. L.; Pecharman, A. F.; Hollis, E.; Yahia, A.; Maron, L.; Parsons, S.; Love, J. B. *Nat. Chem.* **2010**, *2*, 1056.
- (10) Sarsfield, M. J.; Helliwell, M. *J. Am. Chem. Soc.* **2004**, *126*, 1036.
- (11) Arnold, P. L.; Pécharman, A. F.; Lord, R. M.; Jones, G. M.; Hollis, E.; Nichol, G. S.; Maron, L.; Fang, J.; Davin, T.; Love, J. B. *Inorg. Chem.* **2015**, *54*, 3702.
- (12) Rios, D.; Michelini, M. C.; Lucena, A. F.; Marçalo, J.; Gibson, J. K. *J. Am. Chem. Soc.* **2012**, *134*, 15488.
- (13) Lucena, A. F.; Odoh, S. O.; Zhao, J.; Marçalo, J.; Schreckenbach, G.; Gibson, J. K. *Inorg. Chem.* **2014**, *53*, 2163.
- (14) Gong, Y.; Vallet, V.; Michelini, M. C.; Rios, D.; Gibson, J. K. *J. Phys. Chem. A* **2014**, *118*, 325.
- (15) Heinemann, C.; Schwarz, H. *Chem.—Eur. J.* **1995**, *1*, 7.
- (16) Zhou, M. F.; Andrews, L. *J. Chem. Phys.* **1999**, *111*, 11044.
- (17) Hunt, R. D.; Yustein, J. T.; Andrews, L. *J. Chem. Phys.* **1993**, *98*, 6070.
- (18) Andrews, L.; Wang, X. F.; Lindh, R.; Roos, B. O.; Marsden, C. J. *Angew. Chem., Int. Ed.* **2008**, *47*, 5366.
- (19) Fortier, S.; Wu, G.; Hayton, T. W. *J. Am. Chem. Soc.* **2010**, *132*, 6888.
- (20) King, D. M.; Tuna, F.; McInnes, E. J. L.; McMaster, J.; Lewis, W.; Blake, A. J.; Liddle, S. T. *Science* **2012**, *337*, 717.
- (21) King, D. M.; Tuna, F.; McInnes, E. J. L.; McMaster, J.; Lewis, W.; Blake, A. J.; Liddle, S. T. *Nat. Chem.* **2013**, *5*, 482.
- (22) Rios, D.; Rutkowski, P. X.; Shuh, D. K.; Bray, T. H.; Gibson, J. K.; Van Stipdonk, M. J. *J. Mass Spectrom.* **2011**, *46*, 1247.
- (23) Rutkowski, P. X.; Michelini, M. C.; Gibson, J. K. *J. Phys. Chem. A* **2013**, *117*, 451.
- (24) Rutkowski, P. X.; Michelini, M. C.; Bray, T. H.; Russo, N.; Marçalo, J.; Gibson, J. K. *Theor. Chem. Acc.* **2011**, *129*, 575.
- (25) Rios, D.; Michelini, M. C.; Lucena, A. F.; Marçalo, J.; Bray, T. H.; Gibson, J. K. *Inorg. Chem.* **2012**, *51*, 6603.
- (26) Adamo, C.; Barone, V. *J. Chem. Phys.* **1999**, *110*, 6158.
- (27) Cao, X. Y.; Dolg, M.; Stoll, H. *J. Chem. Phys.* **2003**, *118*, 487.
- (28) Cao, X. Y.; Dolg, M. *THEOCHEM* **2004**, *673*, 203.
- (29) Dunning, T. H. *J. Chem. Phys.* **1989**, *90*, 1007.
- (30) Kendall, R. A.; Dunning, T. H.; Harrison, R. J. *J. Chem. Phys.* **1992**, *96*, 6796.
- (31) Woon, D. E.; Dunning, T. H. *J. Chem. Phys.* **1993**, *98*, 1358.
- (32) Valiev, M.; Bylaska, E. J.; Govind, N.; Kowalski, K.; Straatsma, T. P.; Van Dam, H. J. J.; Wang, D.; Nieplocha, J.; Apra, E.; Windus, T. L.; de Jong, W. *Comput. Phys. Commun.* **2010**, *181*, 1477.
- (33) Lide, D. R. *Handbook of Chemistry and Physics*, 90th ed.; CRC Press: Boca Raton, FL, 2009.
- (34) Dewet, J. F.; Dupreez, J. G. H. *J. Chem. Soc. Dalton* **1978**, 592.
- (35) Paine, R. T.; Ryan, R. R.; Asprey, L. B. *Inorg. Chem.* **1975**, *14*, 1113.
- (36) Wright, A. M.; Hayton, T. W. *Comment. Inorg. Chem.* **2012**, *33*, 207.
- (37) Siladke, N. A.; Meihaus, K. R.; Ziller, J. W.; Fang, M.; Furche, F.; Long, J. R.; Evans, W. J. *J. Am. Chem. Soc.* **2012**, *134*, 1243.
- (38) Gendron, F.; Le Guennic, B.; Autschbach, J. *Inorg. Chem.* **2014**, *53*, 13174.
- (39) Evans, W. J.; Fang, M.; Bates, J. E.; Furche, F.; Ziller, J. W.; Kiesz, M. D.; Zink, J. I. *Nat. Chem.* **2010**, *2*, 644.
- (40) Glendening, E. D.; Landis, C. R.; Weinhold, F. *Wires Comput. Mol. Sci.* **2012**, *2*, 1.
- (41) Gong, Y.; Wang, X. F.; Andrews, L.; Schloder, T.; Riedel, S. *Inorg. Chem.* **2012**, *51*, 6983.
- (42) Gong, Y.; Andrews, L. *Dalton Trans.* **2011**, *40*, 11106.
- (43) Kushto, G. P.; Souter, P. F.; Andrews, L. *J. Chem. Phys.* **1998**, *108*, 7121.
- (44) Jacox, M. E.; Thompson, W. E. *J. Chem. Phys.* **1990**, *93*, 7609.
- (45) Lias, S. G.; Bartmess, J. E.; Liebman, J. F.; Holmes, J. L.; Levin, R. D.; Mallard, W. G. *J. Phys. Chem. Ref. Data* **1988**, *17*, 1.